Critical Slowing in Lipid Bilayers

W. Schrader, S. Halstenberg, R. Behrends, and U. Kaatze*

Drittes Physikalisches Institut, Georg-August-Universität, Bürgerstrasse 42-44, 37073 Göttingen, Germany

Received: May 23, 2003; In Final Form: September 23, 2003

Ultrasonic attenuation spectra (100 kHz to 2 GHz) and complex dielectric spectra (300 kHz to 40 GHz) of aqueous solutions of 1,2-dimyristoyl-L-3-phosphatidylcholine vesicles are reported and are discussed in view of their behavior near the main phase transition of the lipid. The relaxation terms in the spectra are assigned to the domain structure fluctuations of the membranes, the structural isomerization of alkyl chains, the axial diffusion of lipid molecules within the membrane, and the reorientational motions of the zwitterionic phospholipid headgroups. The relaxation times of the alkyl chain isomerization and of the headgroup motions on the bilayer surfaces show a steplike change at the transition temperature, T_m. The axial diffusion and the domain fluctuations exhibit substantial effects of slowing near T_m as characteristic for critically demixing liquids at their consolute point.

1. Introduction

During the past decades considerable attention has been directed toward phospholipid bilayer vesicles because these systems are widely accepted models that simulate aspects of biomembrane structure and functions.[1] A multitude of experimental, theoretical, and computer simulation studies has been performed, resulting in a rather comprehensive and sophisticated picture of bilayers. In particular, the main phase transition, at which the membranes change from a solidlike ordered ("gel") phase into a liquidlike disordered ("fluid") phase, accompanied by the melting of the lipid hydrocarbon chains, has been the focus of intense scientific debates. It appears that this main phase transition of the membrane occurs in the vicinity of a critical point. Near the phase transition temperature, T_m, membranes thus exhibit thermodynamic fluctuations over wide ranges of length scales, extending from molecular dimensions to mesoscopic scales.[2] Such fluctuations are believed to be essential for the function of living systems.[3]

At temperatures around T_m, a one-compound phospholipid bilayer presents itself as a distribution of domains of molecules with conformationally disordered chains in a conformationally ordered gel phase and vice versa.[4,5] In correspondence with the microheterogeneous structure of critically demixing liquids near their consolute point, the individual lipid domain size fluctuates rapidly. However, the average domain size is an equilibrium property[6] that varies strongly with the scaled temperature, $t = |T - T_m|/T_m$. It has been suggested that any membrane process that proceeds on length scales smaller than or comparable with the domain size is influenced by the order−disorder fluctuations. Hence the domain structure participates in the control of biological functions associated with membranes.[7] For this reason, it is particularly interesting to gain deeper insights into the lateral dimensions and the microdynamics of the domain structure and into the kinetics of conformer formations of the membrane molecules as well.

Beyond biological implications, domain structure fluctuations of membranes add a special feature to the widely discussed critical point phenomena.[8,9] A particularly appealing aspect is the crossover effects from interrelations between the critical fluctuations and elementary chemical processes, such as structural isomerizations, lateral diffusion, and reorientational motions. We thus found it interesting to compare the relaxation phenomena appearing in broadband ultrasonic spectra of lipid bilayer systems to those displayed by dielectric spectra.

Ultrasonic spectrometry is a powerful method to measure the relaxation rate of order parameter fluctuations of critically demixing binary liquids near their consolute point and to also investigate the kinetics of elementary processes. It has been widely applied to lipid bilayer systems in the past.[10−20] Most studies suffered, however, from a too small frequency band in the measurements, entailing the evaluation of spectra in terms of a single relaxation process with discrete relaxation time. More recently, it was found that in the frequency range from 1 MHz to 3 GHz the ultrasonic spectra reflect a superposition of three relaxation terms of which one seems to be subject to a considerable relaxation time distribution.[19] Recent spectra of aqueous solutions of vesicles from 1,2-dimyristol-L-3-phosphatidycholine,[21] measured between 100 kHz and 2 GHz, indicated this term to be due to critical fluctuations in the domain structure of the membranes near T_m. In this paper, we discuss the relaxation times of order parameter fluctuations, which reveal power law behavior, and the fluctuation correlation length, which may be identified with the average domain size. We also inspect the relaxation parameters of the other terms and compare the relaxation times to such from dielectric spectrometry.

2. Experimental Evidence

Ultrasonic Spectra. Ultrasonic attenuation spectra of aqueous solutions of vesicles from 1,2-dimyristoyl-L-3-phosphatichylcholine (DMPC) had been measured using lipid from Sigma and Fluka (both Deisenhofen, FRG), as well as from Avanti Polar Lipids (Birmingham, AL). No differences exceeding the statistical experimental errors were noticed if the samples were prepared with DMPC from different batches or even different suppliers. Finally, two series of measurements were performed at DMPC concentrations 2 and 10 mg/mL.[21] An extrusion method was applied to obtain a suspension of large unilamellar vesicles with comparatively small size distribution. The mean vesicle diameter $d = (80 \pm 10)$ nm was measured using a photon correlation technique. The phase transition temperature, $T_m =$

10.1021/jp0306489 CCC: $25.00
Published on Web 12/03/2003

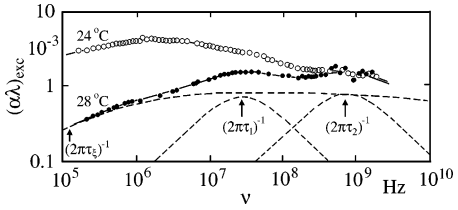

Figure 1. Ultrasonic excess attenuation per wavelength plotted vs frequency for an aqueous solution of extruded DMPC vesicles (lipid concentration 10 mg/mL) at 24 and 28 °C. For the latter spectrum, the subdivision into a Bhattacharjee−Ferrell term (relaxation time τ_ξ) and two Debye terms (relaxation times τ_1, τ_2) is shown by dashed lines.

(24.0 ± 0.1) °C, was determined by sound velocity measurements.[22] In the frequency range from 100 kHz to 2 GHz, ultrasonic attenuation spectra of the samples were recorded at 13 temperatures from 15 to 32 °C using two different methods and seven cells,[21] each matched to a particular frequency range. Due to the overlaps in the frequency ranges of different apparatus and cells, systematic errors in the attenuation coefficient values are most unlikely. In Figure 1, two examples of attenuation spectra are displayed in the format $(\alpha\lambda)_{exc}$ versus frequency, ν. Here $\lambda = c_s/\nu$, c_s = sound velocity, is the sonic wavelength. Excess data,

$$(\alpha\lambda)_{exc} = \alpha\lambda - B\nu \tag{1}$$

are shown, because the asymptotic high-frequency contribution is of less interest here. The excess spectrum at 28 °C clearly reveals contributions from three relaxation processes of which two appear by relative maxima in the $(\alpha\lambda)_{exc}$ data. The other one obviously extends over a significantly broader frequency range, indicating a substantial distribution of relaxation times. At 24 °C, the low-frequency attenuation data are enhanced by a factor of about 10 with respect to those at 28 °C.

It was found that the experimental $\alpha\lambda$ data can be favorably represented by the spectral function ($\omega = 2\pi\nu$)

$$S(\nu) = A_{BF}F_{BF} + \frac{A_1\omega\tau_1}{1+\omega^2{\tau_1}^2} + \frac{A_2\omega\tau_2}{1+\omega^2{\tau_2}^2} + B\nu \tag{2}$$

in which the terms with amplitudes A_i, $i = 1, 2$, denote Debye-type terms.[21] Such terms are characteristic of thermally activated elementary processes in which the educts and products are separated by a potential barrier. The first term on the right-hand side of eq 2 represents a Bhattacharjee−Ferrell (BF) term of critical fluctuations with the amplitude A_{BF} and the scaling function[23]

$$F_{BF}(\nu,T) = F_{BF}(\Omega) = \frac{3}{\pi}\int_0^\infty \frac{x\,dx}{(1+x)^2}\frac{\Omega x(1+x)^{1/2}}{x^2(1+x)+\Omega^2} \tag{3}$$

Here $\Omega = \omega\tau_\xi$ is the reduced frequency with τ_ξ denoting the relaxation time of order parameter fluctuations. According to the dynamic scaling hypothesis[24]

$$\tau_\xi = \xi^2/2D \tag{4}$$

is given by the correlation length ξ of local fluctuations and the diffusion coefficient. Originally, the BF model has been designed to describe the effects of concentration fluctuations of binary critically demixing liquids near their consolute point. It has been shown theoretically, however, that it also applies for the domain structure fluctuations of quasi-two-dimensional lipid membranes.[21] In the numerical calculations, the integral (eq 3) has been represented by the empirical form[25]

$$F_{BF}(\Omega) = \left(\frac{2}{\Omega}\right)^{1/2}[(1+\Omega^2)^{1/4}\cos(0.5\arctan\Omega) - 1] \tag{5}$$

The results from a nonlinear least-squares regression analysis of the spectra in terms of the spectral function (eq 2), treating the relaxation amplitudes and relaxation times, as well as B, as adjustable parameters, have been presented previously in tabular form.[21]

If the spectral function defined by eq 2 is used to represent the ultrasonic attentuation spectra, all relaxation times of the analytical model exhibit slowing characteristics near the phase transition temperature T_m of the DMPC bilayer. As will be detailed discussed below, the high-frequency Debye term ("2" in eq 2) likely reflects the rotational isomerization of the lipid alkyl chains. Such unimolecular reaction is expected to display a steplike change at T_m rather than indications of critical slowing. We thus tried to represent the broadband ultrasonic spectra using various other relaxation spectral models. No function with number of parameters less than eq 2 was found sufficient to represent the experimental spectra within the limits of errors. At least a relaxation term with underlying broad relaxation time distribution is required to account for the existence of excess attenuation in an extended frequency range (Figure 1). Two additional relaxation terms are absolutely necessary for the modeling of the relative maxima in the $(\alpha\lambda)_{exc}$ spectra. Hence only an extension of the $S(\nu)$ function is suitable as an alternative analytical model. We found the spectral function

$$S^{\#}(\nu) = S(\nu) + \frac{A_o\omega\tau_o}{1+\omega^2{\tau_o}^2} \tag{6}$$

a useful description of the measured spectra. The parameters of this function with additional Debye term ("o") are given in Table 1. These parameter values have been also obtained from a least-squares fitting procedure.

The additional low-frequency Debye term adopts non-vanishing amplitudes A_o only at temperatures near T_m. Nevertheless, taking this term into account avoids the slowing characteristics in the high-frequency Debye term ("2") which, as mentioned before, may be questioned for physical reasons. The temperature dependence of the other relaxation times agrees qualitatively for both spectral functions. This result is illustrated by Figure 2 where, as an example, the τ_1 values are displayed to show the small effects from the additional relaxation term on the relaxation times outside the transition region near T_m. The difference between the τ_1 data from the two model relaxation functions may be taken to show the variance in the relaxation times extracted from the experimental spectra.

Dielectric Spectra. As illustrated by Figure 3, the complex dielectric spectra

$$\epsilon(\nu) = \epsilon'(\nu) - i\epsilon''_d(\nu) \tag{7}$$

of purified DMPC solutions with small ion content in the frequency range between 1 MHz and 40 GHz display two dispersion/dielectric loss regions[27] ($d\epsilon'(\nu)/d\nu < 0$, $\epsilon''_d(\nu) > 0$). The dielectric loss

$$\epsilon''_d(\nu) = \epsilon''(\nu) - \sigma/(\epsilon_0\omega) \tag{8}$$

is shown, which results from the total loss, $\epsilon''(\nu)$, by subtraction of the (small) contribution from the dc electric conductivity. The eq 8 ϵ_0 is the electric field constant, and σ is the specific

TABLE 1: Parameters of the Extended Spectral Function $S^{\#}(\nu)$ Defined by Eq 6 for Two DMPC Vesicle Solutions of Different Lipid Concentration c and Sound Velocity c_s as Follows from the Series of Resonance Frequencies of Cavity Resonators Filled with the Samples[21]

T, °C	c, mg/mL	A_{BF}, 10^{-3}, ±5%	Γ, μs^{-1}, ±15%	A_1, 10^{-3}, ±30%	τ_1, ns, ±25%	A_2, 10^{-3}, ±30%	τ_2, ns, ±25%	A_o, 10^{-3}, ±30%	τ_o, ns, ±25%	B, ps, ±1.5%	c_s, m/s, ±0.5%
15.0	10	2.4	0.62	0.2	14	0.7	0.84			46.2	1468.0
18.0	2	0.5	0.31	0.1	12	0.2	0.75			39.5	1476.0
20.0	10	3.7	0.12	0.15	11	0.9	0.70			38.6	1482.6
22.0	2	0.9	0.04	0.13	12	0.5	0.50	0.21	48	34.8	1488.3
23.5	10	4.7	0.01	2.0	13.4	2.5	0.20	5.1	98	34.3	1492.3
24.0	10	5.0	0.001	3.5	21	3.5	0.12	3.4	144	32.5	1493.7
24.5	10	4.0	0.006	4.8	22	4.2	0.105	2.4	149	32.2	1494.0
25.0	2	0.8	0.08	0.8	21	1.0	0.095	0.3	140	31.9	1497.0
26.0	2	0.8	0.25	0.4	20	0.1	0.11			31.3	1499.1
27.0	2	0.7	0.5	0.2	13	1.1	0.09			30.0	1501.7
28.0	10	2.4	0.8	1.2	5.4	4.1	0.09			30.3	1503.1
30.0	2	0.3	0.5	0.2	5.1	0.8	0.1			27.8	1509.0
32.0	10	0.9	0.6	1.2	2.4	4.3	0.1			27.7	1512.5

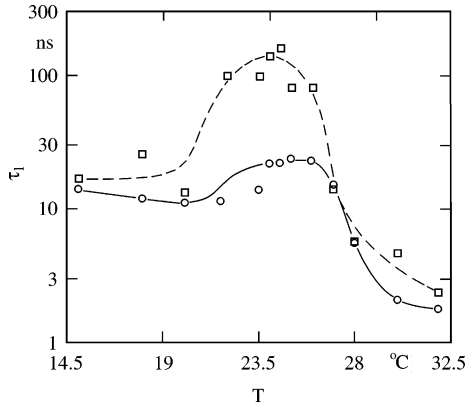

Figure 2. Relaxation times τ_1 following if the measured ultrasonic spectra are fitted to the original function S (□, eq 2, ref 21) and to the extended model spectral function $S^{\#}$ (○, eq 6, Table 1).

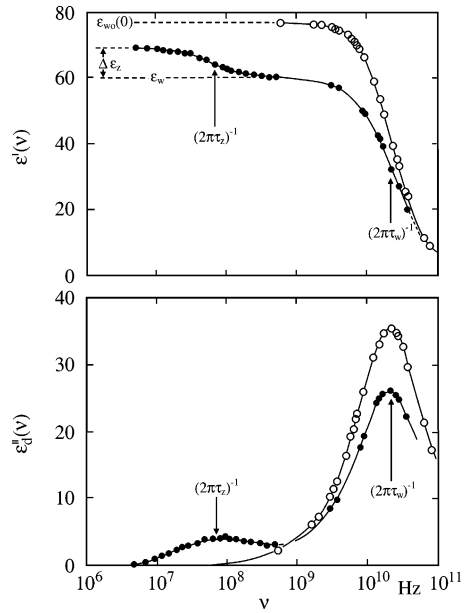

Figure 3. Real part, ϵ' (full symbols), and dielectric contribution, ϵ''_d, to the negative imaginary part of the complex electric permittivity plotted versus frequency for an aqueous DMPC solution (●, lipid concentration 100 mg/mL) and for water (○)[26] at 30 °C.

conductivity. The conductivity of the DMPC solution varied between $(1.03 \pm 0.03) \times 10^{-3}$ S/m at 18 °C and $(1.52 \pm 5) \times 10^{-3}$ S/m at 31 °C. At such σ values, relaxation processes due to limited motions of ions, which have been comprehensively

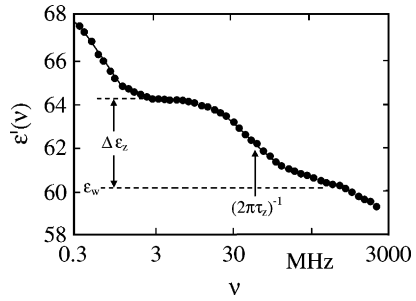

Figure 4. Real part of the dielectric spetrum of a DMPC solution (lipid concentration 60 mg/mL) at 31 °C. Toward low frequencies ($\nu < 3$ MHz), polarizations due to restricted motions of ions contribute to the spectrum.

studied previously,[28,29] contribute to the spectra at even lower frequencies and can thus be easily separated from the high-freqency relaxation terms with relaxation frequencies $\nu_z = (2\pi\tau_z)^{-1}$ and $\nu_w = (2\pi\tau_w)^{-1}$. At the highest temperature of measurements and thus largest σ value, part of the ϵ' spectrum of the DMPC solution is displayed in Figure 4 to show that the high-frequency part of the spectrum ($\nu > 1$ MHz) is not affected by the low-frequency ion processes.

Because we are interested in the high-frequency part of the dielectric spectra here, the complex permittivity data at $\nu > 1$ MHz have been analytically represented by the relaxation function

$$R_d(\nu) = \epsilon(\infty) + \frac{\Delta\epsilon_w}{1 + i\omega\tau_w} + \frac{\Delta\epsilon_z}{1 + (i\omega\tau_z)^{(1-h_z)}} \qquad (9)$$

In this function $\epsilon(\infty)$ denotes the limiting high-frequency contribution, mainly due to electronic and atomic polarization. The second term on the right-hand side of eq 9 describes the relaxation of the water with relaxation frequency $(2\pi\tau_w)^{-1} \approx 22$ GHz at 30 °C. Interactions of water with DMPC molecules are restricted to the dipolar headgroup of the lipid. Therefore the effect of solute/solvent interaction in the overall relaxation time τ_w of the water in the vesicle solutions is small and is, in addition, largely masked by effects from internal fields due to the dielectrically heterogeneous structure of the samples. We shall thus discuss the second relaxation term ("z") only. It is assigned to the reorientational motions of the zwitterions on the bilayer surfaces. This term is subject to a relaxation time distribution, which is, however, much less marked than that of the BF term in the ultrasonic spectra. The relaxation time distribution has been considered by an empirical Cole−Cole

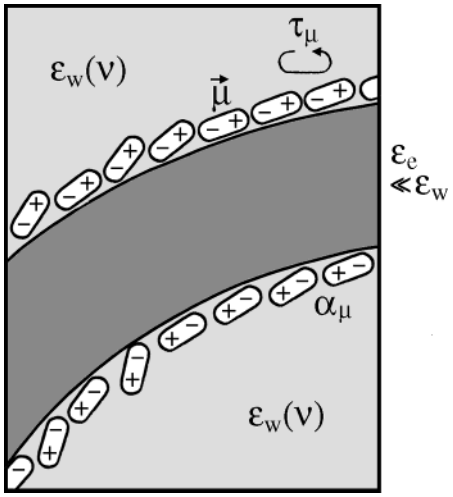

Figure 5. Sketch of the dielectrically heterogeneous vesicle solutions.

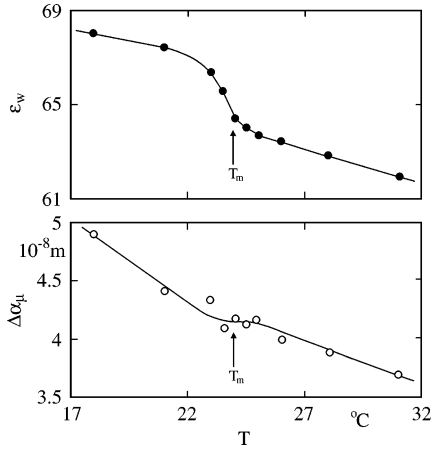

Figure 6. Contribution $\epsilon_w = \epsilon(\infty) + \Delta\epsilon_w$ to the static permittivity (Figures 3 and 4) and surface polarizability amplitude $\Delta\alpha_\mu$ due to the dipolar lipid headgroups (Figure 5) for a DMPC solution (60 mg/mL) displayed versus temperature T.

distribution function, $G(\tau)$, which, when $\tau G(\tau)$ is plotted versus $\ln(\tau/\tau_z)$, is symmetrically bell-shaped. Parameter h_z controls the width of the distribution. For the DMPC solution (60 mg/mL), the parameter values of the zwitterion relaxation term are given in ref 27 at several temperatures around T_m.

The vesicle solutions possess a dielectrically heterogeneous structure (Figure 5), consisting of the bilayer hydrocarbon part with permittivity $\epsilon_e \approx 2$, the phospholipid headgroup regions with surface polarizability α_μ due to the zwitterion dipole moments μ, and water with permittivity $\epsilon_w(\nu)$. The parameters of the R_d function and also the macroscopically determined conductivity, therefore, reflect structural properties of the subphases. The considerable reduction in the water contribution

$$\epsilon_w = \epsilon(\infty) + \Delta\epsilon_w \tag{10}$$

to the static permittivity of vesicle systems (Figure 3) with respect to the pure water static permittivity, $\epsilon_{wo}(0)$, results for the most part from effects of depolarizing electric fields within the dielectrically heterogeneous mixtures. The internal fields have been treated in previous papers,[28,29] allowing us to calculate the water core radius, r_w, of the vesicles from parameter ϵ_w. As discussed in detail in ref 27, the temperature-dependent ϵ_w data, with a steplike change at T_m (Figure 6), correspond with r_w values that increase from 87 nm at 18 °C to 170 nm at 31 °C, thus indicating swelling of the vesicles when T exceeds T_m. Also

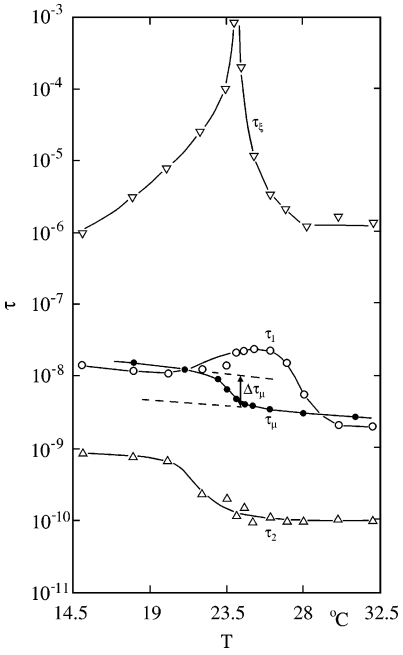

Figure 7. Relaxation times of DMPC vesicle solutions as a function of temperature.

shown in Figure 6 are the amplitudes $\Delta\alpha_\mu$ of the surface polarization, which in the framework of the model of dielectrically heterogeneous solutions results from the relaxation amplitudes $\Delta\epsilon_z$. At T_m, the $\Delta\alpha_\mu$ values show only small effects due to the change of the membrane from the ordered to the disordered phase. Here we are predominantly interested in the microdynamics of the bilayer vesicle solutions. Because the macroscopic relaxation time τ_z of the zwitterion term in $R_d(\nu)$ may somewhat differ from the relaxation time τ_μ of the dipolar lipid headgroups because of the heterogeneous structure of the solutions, the τ_μ values will be used in the following discussion. These values have been also calculated according to the previous theoretical model[28] to appropriately consider the effects from internal electric fields.

3. Discussion

Critical Domain Structure Fluctuations. In Figure 7, the relaxation times from the ultrasonic attenuation spectra are compared to the dipole relaxation time τ_μ measured dielectrically. Near the main phase transition temperature T_m the relaxation time τ_ξ of the domain structure fluctuations increases significantly when approaching T_m, where values on the order of milliseconds or even larger are reached. This slowing had been verified by additional measurements[21] in which the scaling function[23]

$$F_{BF}(\Omega) = \frac{\alpha\lambda(T) - (\alpha\lambda)_{bg}(T)}{\alpha\lambda(T_m) - (\alpha\lambda)_{bg}(T_m)} \tag{11}$$

was determined at various temperatures near T_m. Measurements at low frequencies ($\nu < 1.8$ MHz), where the critical part predominates in the attenuation spectra, had been performed for this purpose. In eq 11, $(\alpha\lambda)_{bg}$ denotes the noncritical background contribution to the spectra. According to the relation

$$(\alpha\lambda)_{bg} = \sum_{j=J}^{2} \frac{A_j\omega\tau_j}{1 + (\omega\tau_j)^2} + B\nu \tag{12}$$

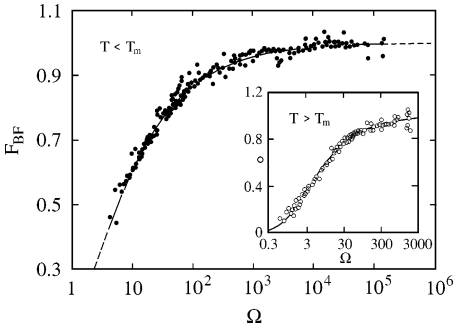

Figure 8. Normalized sonic attenuation coefficient excluding noncritical background contributions (eqs 11 and 12) for a DMPC solution (10 mg/mL) at $T < T_m$ (inset $T > T_m$) shown as a function of reduced frequency. Lines represent the scaling function defined by eq 5.

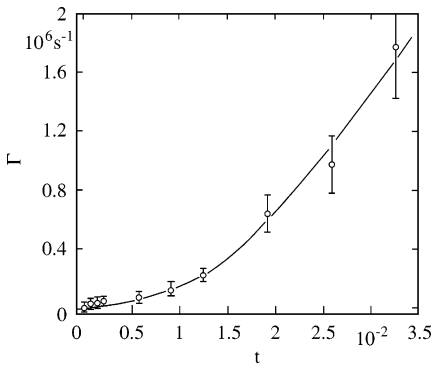

Figure 9. Relaxation rate of domain structure fluctuations at $T > T_m$ vs reduced temperature. The line is the graph of the power law (eq 13) with $\Gamma_o = 1.2(1) \times 10^9\ s^{-1}$.

with $J = 1$, the background contribution had been calculated with the parameters from broadband attenuation spectra (Table 1). To account for the extended relaxation spectral model $S^{\#}(\nu)$, we have reevaluated the experimental data using $J = 0$. Additionally, we considered the temperature denpendence in the sound velocity c_s and the amplitude A_{BF} of the Bhattacharjee−Ferrell term and found the measured $F_{BF}(\Omega)$ data to excellently agree with the empirical form (eq 5) of the scaling function (Figure 8). This agreement has been reached by treating, at each temperature of measurements, the relaxation rate, $\Gamma = \tau_\xi^{-1}$, of domain fluctuations, for both the gel and the fluid phase, as an adjustable parameter. As illustrated by the $\Gamma(t)$ values at $T > T_m$ in Figure 9, the relaxation rates display power law behavior

$$\Gamma(t) = \Gamma_o t^{Z_o\tilde{\nu}} \tag{13}$$

with the exponent $Z_o\tilde{\nu} = 1.93$ that is theoretically predicted for critically demixing binary liquids.[30] Here Z_0 (= 3.05) denotes the universal dynamical exponent and $\tilde{\nu}$ (= 0.63) the universal exponent of the fluctuation correlation length

$$\xi = \xi_0 t^{-\tilde{\nu}} \tag{14}$$

with amplitude ξ_0. When relation 4 and $D = 3 \times 10^{-11}\ cm^2\ s^{-1}$ at $T < T_m$, as well as $D = 7 \times 10^{-9}\ cm^2\ s^{-1}$ at $T > T_m$ (ref 31), are used, fluctuation correlation length values on the order of 10 nm follow from the relaxation times $\tau_\xi = \Gamma^{-1}$ near T_m.

The D values used here for the diffusion of the domains are somewhat smaller than the mass diffusion coefficients of the lipid molecules, for which values between 10^{-10} and $10^{-8}\ cm^2\ s^{-1}$ are reported at $T < T_m$ and $T > T_m$, respectively.[32] In our estimation of correlation length data, we did not consider critical effects in the diffusion coefficient. Therefore, the ξ values should not be overemphasized. Nevertheless, the conclusion may be drawn that only close to T_m the mean size of the domains exceeds the distance d_n of neighboring lipid molecules in the bilayer, which is $d_n = 0.38$ nm at $T < T_m$ and $d_n = 0.45$ nm at $T > T_m$.

Chain Conformational Isomerization. At temperatures above the transition region, the relaxation time τ_2 of the high-frequency Debye-type relaxation term in the ultrasonic spectra (Figure 7) corresponds to the correlation times of terminal end groups of the lipid chains (10^{-11}−10^{-10}s) and of segmental motions in the middle of the chain (10^{-9} s) in a membrane, as measured by NMR studies of specifically deuterium-labeled systems.[33] It nicely agrees with the relaxation time in the ultrasonic and shear viscosity spectra of *n*-tetradecane (0.19 ns, 25 °C) and of other liquid *n*-alkanes of similar length.[34] The fast relaxation of alkanes has been shown to reflect a collective mode of chain isomerization, which is controlled by the length of the molecules. Obviously, by analogy with the chains in the core of micelles,[35] similar isomerizations occur in the fluid phase of lipid bilayers. In the gel phase, the relaxation time is larger (Figure 7), indicating the reduced mobility in the chain structural isomerization due to the solidlike order of the membranes.

The ultrasonic relaxation of *n*-alkanes had been considered in terms of a coupled torsional oscillator model,[36,37] which predicts a series of relaxation terms. If we assume the high-frequency Debye term to correspond with the first normal mode of coupled torsional oscillators, representing the transition between the all-trans conformation of chains to a conformation with k rotated C−C bonds, the relaxation rate

$$\tau_2^{-1} = 2\nu_0 \sin^2\left(\frac{\pi}{2n_0}\right) e^{-\Delta G^{\#}/(RT)} \tag{15}$$

is given by the characteristic frequency ν_0 for the rotation of an individual C−C bond, by the number n_0 of individual torsional oscillators per chain, and by the Gibbs free energy of activation, $\Delta G^{\#}$. Using $\nu_0 = 8.5$ THz as reported for ethane[38] and assuming three hydrocarbon groups in the alkyl chain to form one oscillating unit, that is, $n_0 = n/3$ if n is the number of groups per chain, we find $\Delta G^{\#} = (17.5 \pm 0.5)$ kJ/mol at $T \leq 28$ °C. This value compares with $\Delta G^{\#} = (14.5 \pm 0.5)$ kJ/mol for *n*-tetradecane at 25 °C if again $n_0 = n/3$ is assumed.[34] Hence the torsional oscillator model of chain isomerization applies well to lipid membranes. The relaxation amplitude

$$A_2 = \frac{\pi\Gamma_2 c_\infty^{\,2}\rho}{RT}\Delta V_{ad,2}^{\,2} \tag{16}$$

of the unimolecular reaction

$$Y \rightleftharpoons Y^* \tag{17}$$

is related to the stoichiometric factor

$$\Gamma_2 = [Y][Y^*]/([Y] + [Y^*]) \tag{18}$$

and the isentropic reaction volume

$$\Delta V_{ad,2} = \frac{\mathcal{A}_\infty}{\rho c_{p\infty}}\Delta H + \Delta V \tag{19}$$

In these equations, Y and Y* denote two different chain conformations, c_∞, $c_{p\infty}$, and $\mathcal{A}_\infty$ are the extrapolated high-frequency sound velocity, heat capacity at constant pressure, and thermal expansion coefficient, respectively, ρ is the density,

and ΔH and ΔV are the reaction enthalpy and the isothermal reaction volume. For reasonable reaction enthalpies, on the order of 1 kJ/mol, the ΔH term in eq 19 can be neglected; thus, $\Delta V_{ad,2} = \Delta V$. If ΔV_0 denotes the molar volume change due to the rotation of a single C−C bond and ΔV_h the corresponding volume change in the headgroup region, the mean number

$$k = (\Delta V - \Delta V_h)/\Delta V_0 \tag{20}$$

of rotated bonds per lipid molecule can be calculated from the A_2 values and the stoichiometric parameter

$$\Gamma = c\frac{k(1-k)}{n-1} \tag{21}$$

Assuming $\Delta V_0 = 1.8$ cm^3/mol as follows from the volume change of long *n*-alkanes[39] and $\Delta V_h = 5$ mL/mol, $k/2 = 1.9$ follows for the mean number of rotated bonds per hydrocarbon chain at $T \leq 20$ °C, corresponding with $K_k = 0.6$ kinks per chain. At $T \geq 28$ °C, these numbers are $k/2 = 4.7$ and $K_k = 1.5$. Even though these K_k values are rough estimates only, the increase in the number of kinks by one per chain on exceeding the transition temperature is a quite realistic result. $K_k = 0.1$ for $T < T_m$ and $K_k = 0.6-2.0$ for $T > T_m$ had been derived from volume measurements.[39]

Axial Diffusion. The relaxation time τ_1 of the low-frequency Debye-type relaxation term in the ultrasonic spectra also exhibits a substantial effect of slowing near the phase transition temperature. Around T_m, the τ_1 values correspond with the correlation time for the lateral diffusion of the lipid molecules.[33] Outside this temperature range, however, our relaxation times rather agree with the NMR correlation times $10^{-9}-10^{-8}$ s for the axial diffusion of phospholipid molecules.[33] We thus assume the τ_1 values to reflect the rotational motions of the DMPC molecules within the membrane. Interestingly, at $T \leq 20$ °C and $T \geq 28$ °C these values, within the limits of experimental error, agree with the relaxation times τ_μ for the reorientational motions of the dipolar lipid headgroups as determined from dielectric spectra. Obviously, outside the transition region the rotational motions of the headgroup are coupled to those of the whole molecule. In the transition region, no such degeneration exists. Whereas the axial diffusion of the whole molecule slows down, the reorientations of the dipolar headgroup stepwisely change to distinctly faster motions (Figure 7): $\Delta\tau_\mu/\tau_\mu(T_m) = 1.4$. Obviously, in the transition region and above T_m, the headgroups are able to reorientate almost independently from one another. The axial diffusion of the whole molecules displays characteristics of a collective phenomenon. If we assume that some free volume is required for axial diffusion, a crossover to lateral diffusion processes and an increase in the relaxation time due to slowing of the density fluctuations near T_m likely follows.

Vesicle Deformation? The molecular mechanisms behind the additional low-frequency Debye relaxation term are not clear presently. We suggest the relaxation term with relaxation time τ_o around 0.1 μs to be due to local shape deformations of vesicles. Recent optical measurements of the membrane fluctuations and of the bending rigidity of lipid vesicles have revealed critical behavior of the bending modulus and a vesicle deformation along the optical axis.[40] At 30 °C, a DPPC vesicle (1,2-dipalmitoyl-L-3-phosphatidylcholine, $T_m \approx 41$ °C, diameter = 15 μm) responded to a 53-fN optical force with a relaxation time on the order of seconds. Probably, in the transition region near T_m where the low-frequency Debye relaxation term features a nonvanishing amplitude A_o (Table 1), there exist also short scale deformation modes with fluctuation times as small as τ_o. This assumption, however, has still to be verified by further investigations.

4. Conclusions

Near the main phase transition temperature T_m of DMPC bilayer vesicle solutions, the relaxation rate of the domain structure fluctuations follows power law behavior and reaches values substantially below the available frequency range of ultrasonic spectrometry, thus evidencing aspects of a second-order transition. The fluctuation correlation length, corresponding with the mean domain size, increases when the temperature approaches T_m. The extent of this increase, however, is not well-known because of the insufficient knowledge of the diffusion coefficient near T_m. The structural isomerization of the lipid alkyl chains can be described in terms of a torsional oscillator model in which three hydrocarbon groups form one oscillating unit, a kink. At temperatures above the transition region, the free energy of activation $\Delta G^\#$ of the chain isomerization agrees with that of *n*-tetradecane at 25 °C, indicating close similarity in the motions of hydrocarbon chains in the fluid phase of bilayers and of liquid *n*-alkanes. At temperatures below the transition region, because of the solidlike order of the chains, $\Delta G^\#$ is larger by 3.4 kJ/mol. In the transition region, the axial diffusion of the whole lipid molecule is decoupled from the reorientational motions of the dipolar headgroup, the relaxation time of which is smaller by about 1 order of magnitude. Outside the transition region, the rotational diffusion of the whole molecule and of the headgroup are characterized by identical relaxation times (20 ns at $T \leq 20$ °C; 3 ns at $T \geq 28$ °C). Hence the modes of motions are degenerate. Close to T_m, an additional relaxation process is reflected by the ultrasonic spectra, which has been tentatively assigned to local shape deformations of vesicles.

Acknowledgment. We thank Prof. T. Heimburg and Prof. J. K. Bhattacharjee for much spirited discussions. Financial assistance by the Deutsche Forschungsgemeinschaft is gratefully acknowledged.

References and Notes

(1) Lipowsky, R., Sackmann, E., Eds. *Structure and Dynamics of Membranes*; Elsevier: Amsterdam, 1995; Vol. 1A, From Cells to Vesicles; Vol. 1B, Generic and Specific Interactions.
(2) Nielsen, L. K.; Bjørnholm, T.; Mouritson, O. G. *Nature* **2000**, *404*, 352.
(3) Zhang, R.; Sun, W.; Tristam-Nagle, S.; Headrick, R. L.; Suter, R. M.; Nagle, J. F. *Phys. Rev. Lett.* **1995**, *74*, 2832.
(4) Pedersen, S.; Jørgensen, K.; Bækmark, T. R.; Mouritsen, O. G. *Biophys. J.* **1996**, *71*, 554.
(5) Heimburg, T. *Curr. Opin. Colloid Interface Sci.* **2000**, *5*, 224.
(6) Mouritson, O. G.; Jørgensen, K. *Chem. Phys. Lipids* **1994**, *73*, 3.
(7) Mouritson, O. G.; Jørgensen, K. *Mol. Membr. Biol.* **1995**, *12*, 15.
(8) Fisher, M. E. *Rev. Mod. Phys.* **1998**, *70*, 653.
(9) Stanley, H. E. *Rev. Mod. Phys.* **1998**, *71*, 5358.
(10) Hammes, G. G.; Roberts, P. B. *Biochim. Biophys. Acta* **1970**, *203*, 220.
(11) Eggers, F.; Funck, T. *Naturwissenschaften* **1976**, *63*, 280.
(12) Mitaku, S.; Ikajansi, A.; Sakaniski, A. *Biophys. Chem.* **1978**, *8*, 295.
(13) Gamble, R. C.; Schimmel, P. R. *Proc. Natl. Acad. Sci. U.S.A.* **1978**, *75*, 3011.
(14) Harkness, J. E.; White, R. D. *Biochim. Biophys. Acta* **1979**, *552*, 450.
(15) Mitaku, S. F.; Date, T. *Biochim. Biophys. Acta* **1982**, *688*, 411.
(16) Sano, T.; Tanaka, J.; Yasunaga, T.; Toyoshima, Y. *J. Phys. Chem.* **1982**, *86*, 3013.
(17) Mitaku, S.; Jippo, T.; Kataoka, R. *Biophys. J.* **1983**, *42*, 137.
(18) Strom-Jensen P. R.; Magin, R. L.; Dunn, F. *Biochim. Biophys. Acta* **1984**, *769*, 179.
(19) Kaatze, U.; Brai, M. *Chem. Phys. Lipids* **1993**, *65*, 85.

(20) Morse, R. P. D.; Ma, L. D.; Magin, R. L.; Dunn, F. *Chem. Phys. Lipids* **1999**, *103*, 1.
(21) Halstenberg, S.; Schrader, W.; Das, P.; Bhattacharjee, J. K.; Kaatze, U. *J. Chem. Phys.* **2003**, *118*, 5683.
(22) Lautscham, K.; Wente, F.; Schrader, W.; Kaatze, U. *Meas. Sci. Technol.* **2000**, *11*, 1432.
(23) Ferrell, R. A.; Bhattacharjee, J. K. *Phys. Rev. A* **1985**, *31*, 1788.
(24) Halperin, B. I.; Hohenberg, P. C. *Phys. Rev.* **1969**, *177*, 952.
(25) Bhattacharjee, J. K.; Ferrell, R. A. *Phys. Rev. E* **1997**, *56*, 5.
(26) Ellison, W. J.; Lamkaouchi, K.; Moreau, J. M. *J. Mol. Liq.* **1996**, *68*, 171.
(27) Schrader, W.; Kaatze, U. *J. Phys. Chem. B* **2001**, *105*, 6266.
(28) Pottel, R.; Göpel, K.-D.; Henze, R.; Kaatze, U.; Uhlendorf, V. *Biophys. Chem.* **1984**, *19*, 233.
(29) Tirado, M.; Grosse, C.; Schrader, W.; Kaatze, U. *J. Non-Cryst. Solids* **2002**, *305*, 373.
(30) Anisimov, M. A. *Critical Phenomenon in Liquids and Liquid Crystals*; Gordon and Breach: Philadelphia, PA, 1991.
(31) Korlach, J.; Schwille, P.; Webb, W. W.; Feigenson, G. W. *Proc. Natl. Acad. Sci. U.S.A.* **1999**, *96*, 8461.
(32) Schwille, P.; Korlach, J.; Webb, W. W. *Cytometry* **1999**, *36*, 176.
(33) Smith, R. L.; Oldfield, E. *Science* **1984**, *225*, 280.
(34) Behrends, R.; Kaatze, U. *J. Phys. Chem. A* **2000**, *104*, 3269.
(35) Kaatze, U.; Lautscham, K.; Berger, W. *Z. Phys. Chem. (München)* **1988**, *159*, 161.
(36) Tobolsky, A. V.; DuPrè, D. B. *Adv. Polym. Sci.* **1969**, **6**, 103.
(37) Cochran, M. A.; Jones, P. B.; North, A. M.; Pethrick, R. A. *J. Chem. Soc., Faraday Trans. 2* **1972**, *68*, 1719.
(38) Pitzer, K. S. *J. Chem. Phys.* **1944**, *12*, 310.
(39) Träuble, H.; Haynes, D. *Chem. Phys. Lipids* **1971**, *7*, 324.
(40) Lee, C.-H.; Lin, W.-C.; Wang, J. *Phys. Rev. E* **2001**, *64*, 020901.